1998ASPC..132..220A

Star Formation with the Infrared Space Observatory
ASP Conference Series, Vol. 132, 1998
J. L. Yun, and R. Liseau, eds.

The dense core Oph D seen in extinction by ISOCAM

A. Abergel, J.P. Bernard, F. Boulanger, F.X. Désert, G. Lagache, J. L. Puget and W.T. Reach

Institut d'Astrophysique Spatiale, Université Paris-Sud, Bât.121, 91405, Orsay, France

E. Falgarone

Radioastronomie Millimétrique, Ecole Normale Supérieure, 24 rue Lhomond, 75005 Paris, France

L. Nordh, G. Olofsson

Stockholm Observatory, S-133 36 Saltsjöbaden, Sweden

P. André, A. Bacmann

Service d'Astrophysique, Centre d'Etudes de Saclay, 91191 Gif-Sur-Yvette Cedex, France

I. Ristorcelli

CESR, UPR-CNRS 8002, 9 avenue du colonel Roche, 31029 Toulouse Cedex, France

Abstract. We present a detailed analysis of the dense core Oph D which is one of the most spectacular prestellar cores revealed in extinction by ISOCAM in the ρ Ophiuchi main cloud (Abergel et al. 1996).
Conducted in the two filters LW2 (5-8.5 μm) and LW3 (12-18 μm), the observations confirm the wavelength dependence of the extinction curve for standard graphite-silicate dust grains. Opacity maps are obtained with an unprecedented angular resolution (6 arc sec) and sensitivity. We deduce new estimates of the total mass of the core: M_{TOT}= 7.3-13.9 and 8.4-10.8 $M_\odot$ for the LW2 and LW3 filters respectively.
The density structure of the core edge which has the steepest IR brightness gradient is modeled with a simple spherical geometry. The density profiles strongly depart from a r^{-2} sphere due to a central flattening of the internal regions (typically for $r < 0.02$ pc). Using the over-simplified picture of a core embedded in an external cloud with a constant density fixed to 10^4 H cm^{-3}, we reach the conclusion that the external parts of the profiles are steeper than a r^{-2} law. However r^{-2} density profiles are also compatible with the data since the density outside the core is actually poorly constrained.

© Astronomical Society of the Pacific • Provided by the NASA Astrophysics Data System

1998ASPC..132..220A

1. Introduction

The understanding of the physical properties of dense starless cores is a critical issue in the theory of star formation, since these objects are believed to be stellar progenitors. Because of their very high column density ($N_H > 10^{22}$ cm^{-2}), they are opaque in the visible. The first extensive surveys of dense cores have been conducted using the (J,K) = (1,1) NH_3 emission line by Myers and co-workers (Myers and Benson 1983, Benson and Myers 1989 and references therein). A number of other molecules are now commonly used, such as CS, $C^{18}O$, C_3H_2, DCO^+, HCO^+, $H^{13}CO^+$, ... (see Butner et al. 1995 and references therein). In the ρ Ophiuchi main cloud (L1688), several dense cores have been observed using HCO^+ and DCO^+ emission lines (Loren & Wootten 1986, Loren et al. 1990). Up to now, such observations give estimates of the central column density and the central density of the cores, but not of the density structure because of their limited angular resolution (at least a few 10") and possible excitation and chemistry effects.

Sub-millimeter and millimeter observations allow to detect the continuum emission of starless dense cores. Ward-Thompson et al. (1994) have conducted a survey of several cores, while André et al. (1996) have presented a detailed analysis of the density structure of the prestellar core L1689B based on 1.3 mm continuum mapping conducted at IRAM with the unprecedented angular resolution of 11 arcsec. Both studies suggest that the radial emission profiles are consistent with a power law density $n(r) \alpha r^{-2}$ in the outer regions, but systematically flatten out near the center, at radii less than a few thousands AU. None of the profiles appear consistent with a singular r^{-2} isothermal sphere (Shu 1977). However, to deduce density profiles from the sub-mm and 1.3 mm emission profiles, it has been assumed that the dust temperature and the dust opacity do not vary in the core. These two assumptions are questionable. Starless cores are heated from the outside so the temperature should be lower in the inner parts (see Falgarone and Puget 1985). Moreover, the physical properties of the dust, and as a consequence the opacity of the dust particles, likely vary within the cores (see the review of Henning et al. 1995). The sub-mm and mm observations are also limited by sensitivity in the outer parts so that the density structure at the interface with the ambient molecular cloud is not strongly constrained.

The IR camera ISOCAM of the ISO satellite (Cesarsky et al. 1996) gives a new view on dense cores in several molecular clouds, seen as deep absorption features against a diffuse extended background (Abergel et al. 1996, Bacmann et al. 1997). The main cloud of ρ Ophiuchi (L1688) is ideal to reveal structures in extinction, since it is mainly illuminated from its far side by the Sco OB2 association (de Geus et al. 1989). Moreover it is one of the nearest (160 pc, Bertiau 1958) extended molecular complex located at high Galactic latitude ($b \simeq 17°$). Totally opaque on optical plates, the main cloud is known to contain a few young embedded B stars and extremely numerous Young Stellar Objects (YSOs) previously identified in the near IR (Wilking et al. 1989, Greene & Young 1992). Several deep absorption features due to starless dense cores are detected in the ISOCAM field, together with a large number of absorptions features with a lower contrast (Abergel et al. 1996). This paper presents the first detailed study of one of these dense cores, Oph D (located at α_{2000}=16h28m30s,

© Astronomical Society of the Pacific • Provided by the NASA Astrophysics Data System

1998ASPC..132..220A

δ_{2000}=-24°19'). This core is not included in a region containing strong variations of the brightness at small scales (except a few embedded YSOs, see Fig. 1). Therefore the foreground emissions can be assumed uniform and the background emission deduced by interpolating the brightness measured outside the core.

The constraints on the foreground emission are discussed in section 2, then we derive in section 3 the opacity maps obtained for the two broad-band ISOCAM filters LW2 (5-8.5 μm) and LW3 (12-18 μm) centered to 6.75 and 15 μm respectively. We see in sect 4. that the ratio of the opacities deduced from the two filters are consistent with the presence of the absorption feature at 10 μm due to silicate. The total mass of Oph D is derived from the opacity maps using the Draine & Lee (1984) extinction law of graphite and silicate sphere (sect. 5). The density structure of the core which has the steepest IR brightness gradient is analysed in section 6 using a simple spherical model.

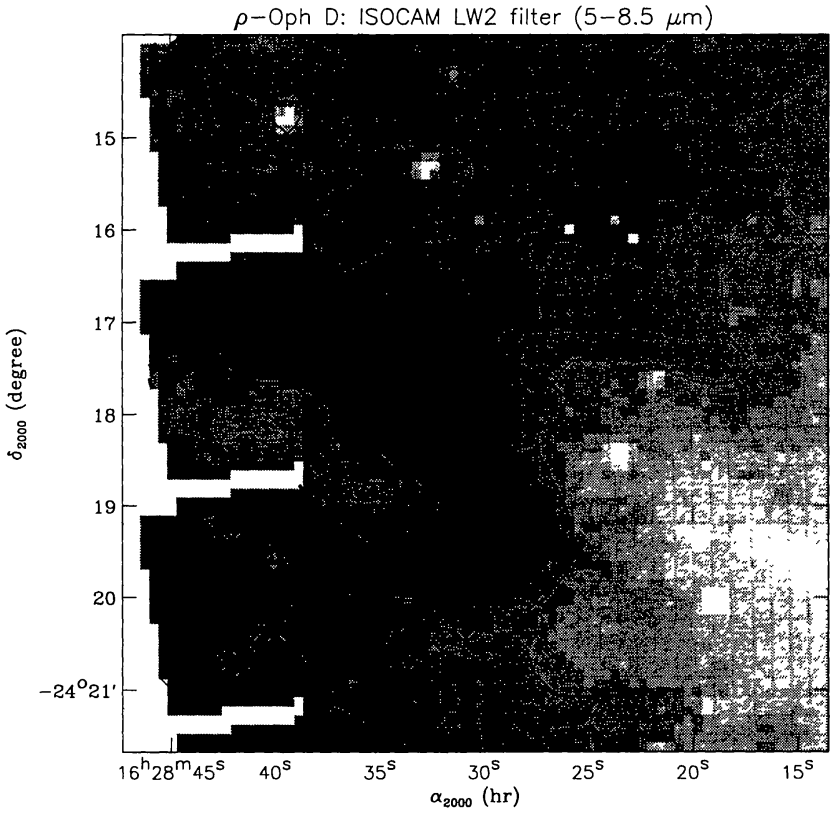

Figure 1. Oph D dense core in the LW2 filter (5-8.5 μm), seen as a dark patch around extended emission. The solid contours are at 4, 5 (thick), 6, 7, 8 MJysr^{-1} (after removing the zodiacal emission, see sect. 2).

© Astronomical Society of the Pacific • Provided by the NASA Astrophysics Data System

1998ASPC..132..220A

2. Foreground emission

The foreground emission is assumed constant. It contains the zodiacal emission and the emission coming from the near side of the dense cloud. To estimate the zodiacal emission, we use the model of Reach et al. (1995) calibrated from the DIRBE/COBE data. This model gives a zodiacal emission equal to 5.7±1 and 45±9 MJysr^{-1} at 6.75 μm and 15 μm respectively (the ecliptic latitude β is around -2.5°) and at the epoch of ISOCAM observations. Our observations of L1688 provide indeed a stronger constraint for the zodiacal emission at 15 μm: 39^{+0}_{-3}MJysr^{-1}, since the minimal brightness is equal 39 MJysr^{-1} (at 6.75 μm, it is equal to 7.4 MJysr^{-1}).
The contribution of the dust located at the near side of the cloud is unknown, but we can use as an upper limit for the total foreground emission the minimal brightness of the core measured in the most absorbed pixels ($I_\nu(6.75\mu m) = 8.4$ and $I_\nu(15\mu m) = 40.1$ MJysr^{-1}). Finally the best estimate for the total foreground emission of Oph D is in the range 5.7-8.4 MJysr^{-1} and 39-40.1 MJysr^{-1} at 6.75 μm and 15 μm respectively.

3. Opacity map of Oph D

The extinction across the core is calculated assuming that :

1. the core is embedded into a cloud with a constant density n_{out} and a typical size L,
2. this cloud is illuminated from its rear side by the intensity I_{back},
3. the foreground emission I_{fore} is constant (we will see in section 5 that I_{fore} is dominated by the zodiacal contribution),
4. the spatial fluctuations of I_{back} at the scale of the core size are negligible.

The emission measured for a line of sight crossing the core and at a sky position (l,b) can be written: $I(l,b) = I_{back}(l,b)\ e^{-N(l,b)\sigma} + I_{fore}$, where σ is the cross section of the dust particles and $N(l,b)$ the total column density of the core and of the cloud containing the core along the line of sight. Let l_{path} be the length of the path of the line of sight inside the core (for a spherical core of radius r_{core}, $l_{path} = 2\sqrt{r^2_{core} - r^2}$, r being the distance from the core centre), and $N_{core}(l,b)$ the column density of the core crossed by the line of sight. We have: $N(l,b) = N_{core}$(l,b) + (L-$l_{path}(l,b))n_{out}$.
Outside the core, $N_{core}(l,b) = 0$ and $l_{path}(l,b) = 0$, thus the emerging intensity is: $I_{out}(l,b) = I_{back}(l,b)\ e^{-Ln_{out}\sigma} + I_{fore}$. As n_{out} is assumed constant, the dependence of I_{out} with the sky position is only due to the large scale spatial fluctuations of I_{back}.
Finally we have: $-\log(\frac{I(l,b)-I_{fore}}{I_{out}(l,b)-I_{fore}}) = (N_{core}(l,b) - l_{path}(l,b)n_{out})\sigma = \Delta\tau(l,b)$, which is the difference of opacity profiles between the core and a core with a constant density equal to n_{out}. In the following we will improperly call the map of $\Delta\tau$ an "opacity map". In the central regions, the opacity of a core with a constant density equal n_{out} is obviously negligible compared to the opacity of

© Astronomical Society of the Pacific • Provided by the NASA Astrophysics Data System

1998ASPC..132..220A

the dense core, but it is not the case near the edge. For lines of sight crossing the core, we have estimated $I_{out}(l, b)$ by interpolating the emission measured out of the core. In practice, a minimal curvature spline surface is fitted to selected sky positions where the extinction is negligible.
Figure 2 presents the opacity map determined from the LW2 emission (τ_{LW2}), the foreground emission being assumed to contain only the zodiacal contribution. An identical map has been obtained from the LW3 emission. The distribution of the column density of the core is revealed with an unprecedented angular resolution and sensitivity. The 0.1 contour of figure 2 is included in a tilted 0.25 pc × 0.16 pc ellipse which contains most of the total mass of the core (see sect. 5).

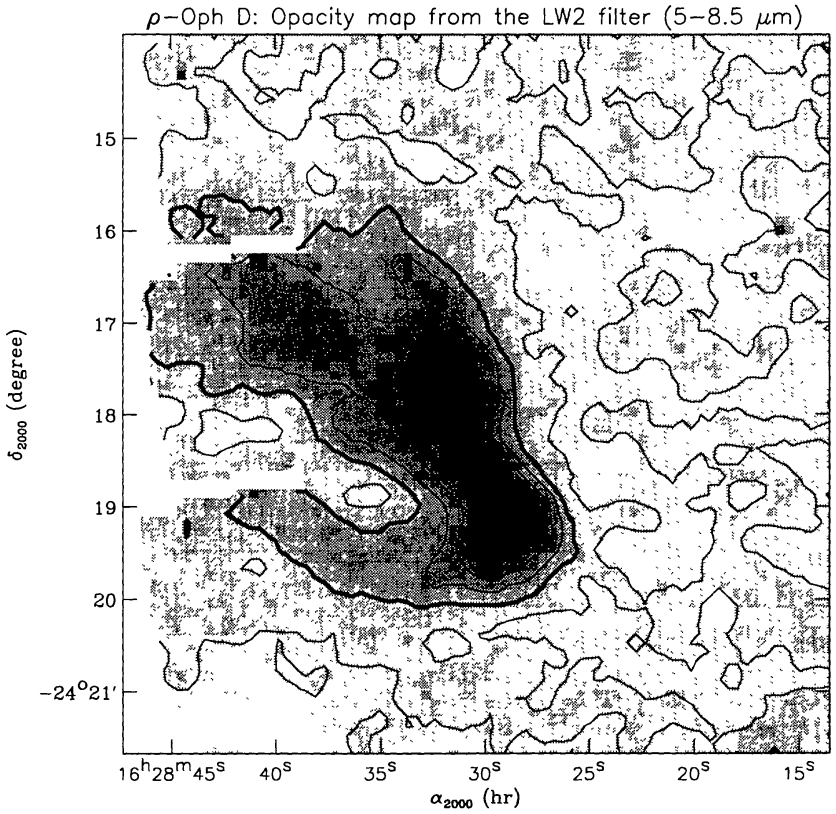

Figure 2. Opacity map deduced from the ISOCAM observations within the LW2 filter. The solid contours are at τ_{LW2}= 0, 0.1 (thick), 0.2, 0.3, 0.5, 0.7, 0.9. At a distance of 160 pc, 1' corresponds to 4.65 10^{-2} pc.

4. Absorption cross section of the dust particles

The absorption cross section of the dust particles located in the core is assumed to be the same as in the surrounding cloud, and estimated using the standard values of Draine & Lee 1984 for graphite and silicate spheres. For the LW2 and the LW3 filters, we have used: $\lambda\tau/N_H$= 5 10^{-27} and 1.5 10^{-26} cm^{-3}/H respec-

© Astronomical Society of the Pacific • Provided by the NASA Astrophysics Data System

1998ASPC..132..220A

tively (the difference between these two values is due to the silicate absorption feature at 10 μm), which gives by taking the nominal wavelength of 6.75 and 15 μm for the two filters a ratio of opacity τ_{LW3} / τ_{LW2}= 1.35.
The Draine & Lee model has been calibrated using several observations of the extinction of stars across diffuse clouds, so the extinction curve may be strongly different for the dust inside dense cores where the local density is typically 1000 times higher than in diffuse clouds. However, preliminary analysis of spectrophotometric observations of Oph D with ISOCAM are consistent with the presence of the silicate feature, since the extinction is significantly higher around the aromatic hydrocarbon features at 11.3 and 12.7 μm than around the features at 7.7 and 8.6 μm (Fig. 3). Moreover, the ratio of the integrated opacity for the two filters is in the range 1-1.5, depending on the assumed foregrounds (see sect. 2). The wavelength dependence of the opacity of Oph D measured by ISOCAM is clearly in favour of the Draine & Lee model. It is inconsistent with the puzzling results of Lutz et al. (1996) which have derived an extinction law toward the galactic centre which does not present any silicate feature, using the recombination lines of hydrogen measured by the SWS experiment of ISO (typically τ_{LW3} / $\tau_{LW2} \simeq 0.5$).

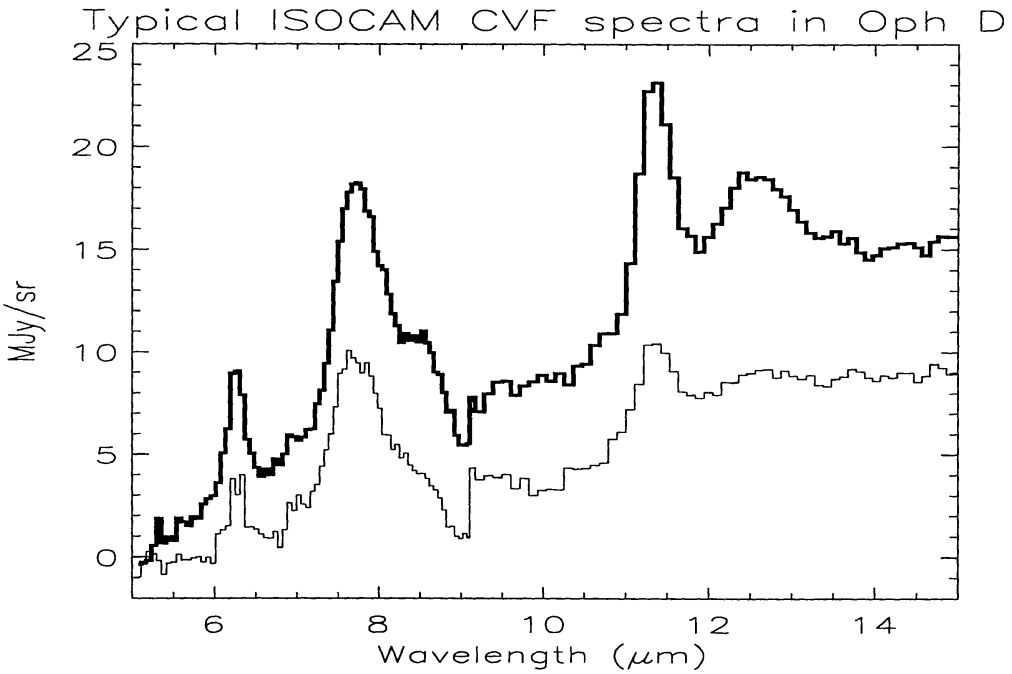

Figure 3. Averaged ISOCAM spectra measured using the long-wavelength Circular Variable Filter (CVF) in and out of Oph D (thick and thin lines respectively). A zodiacal spectrum (Reach et al. 1996) has been removed after proper rescaling. Part of the continuum and the jump around 9.1 μm are due to the preliminary status of the data processing. The two spectra show the 6.2, 7.7, 8.6, 11.3 and 12.7 μm features characteristic of aromatic hydrocarbons.

© Astronomical Society of the Pacific • Provided by the NASA Astrophysics Data System

1998ASPC..132..220A

5. Total mass of Oph D and constrain on the foreground emission

The integral values of the opacity maps allow to derive the total mass of the gas which attenuate the rear side emission. We obtain M_{TOT}= 7.3-13.9 and 8.4-10.8 $M_\odot$ for the LW2 and LW3 filters respectively, the lower (resp. upper) limit being obtained when the foreground emission is equal to the zodiacal (resp. minimal) emission. The range is higher for the LW2 filter than for the LW3 one, due to a higher range for the foreground emission (see sect. 2). The contribution of the gas with a constant density n_{out} equal to the external density should be subtracted from M_{TOT} (see sect. 3). However, this contribution is negligible (typically 0.1 $M_\odot$ for $n_{out} = 10^4$ cm^{-3}, which is the density derived from the ^{13}CO J=1-0 observations of Oph D by Loren 1989).
Our estimates of M_{TOT} are slightly higher than the value of 5.2 $M_\odot$ derived by Butner et al. (1995) from DCO^+ J=1-0 observations. Part of the difference may be due to the higher signal to noise of our observation, since we detect a diffuse extended extinction at the east side of the core (Fig. 2) not detected on the map of Butner et al. If we restrict the core to high opacities regions (τ_{LW2} >0.2), M_{TOT} derived from the LW2 (resp. LW3) opacity is in the range 4.6-9.0 $M_\odot$ (resp. 5.1-6.2 $M_\odot$).
We see that the value of M_{TOT} is identical to the DCO^+ mass if we consider that the foreground emission is only made of the zodiacal contribution. We obtain the same conclusion using the peak opacity of the core: to deduce central column densities consistent with those derived from the DCO^+ observations (and also from observations at 1.3 mm, see Motte et al. 1997), it is necessary to neglect the emission which could come from the near side of the cloud. Therefore in the following, we will consider that the foreground emission is only due to the zodiacal contribution.

6. Density structure

The opacity map of Oph D (Fig. 2) shows that the tri-dimensional shape of the core is complex. One striking characteristic is the east-west asymmetry: the opacity profiles are obviously steeper on the western edge than on the eastern.
The density structure of the western edge is modeled in a spherical geometry: an internal core with a constant local density n_0 up to a radius r_0, and a power law decrease $n(r)=n_0(r_0/r)^\beta$ down to the density of the surrounding gas n_{out}. The model is tested with β= 2 (singular isothermal sphere) and β= 3. The free parameters n_0 and r_0 are adjusted in order to fit the computed opacity profiles with the east-west profiles determined from the data. n_{out} can also be adjusted, or be fixed to the estimated value of 10^4 H cm^{-3} consistent with the ^{13}CO J=1-0 observations of Oph D by Loren (1989). The core radius r_{core} is deduced from n_0 and r_0 with: $n_{out}= n_0(r_0/r_{core})^\beta$.
On figure 4 is presented an example of opacity profile across the core, together with different results of the modeling for the western edge (we have obtained identical conclusions for most of the western profiles crossing the core). The absorption profiles are never saturated. The parameter values are given in table 1. The total width of the profiles is typically 0.1 pc (2.1 arc min). The central part indicates the presence of an internal core with a constant density ($n_0 \sim 10^6$

© Astronomical Society of the Pacific • Provided by the NASA Astrophysics Data System

1998ASPC..132..220A

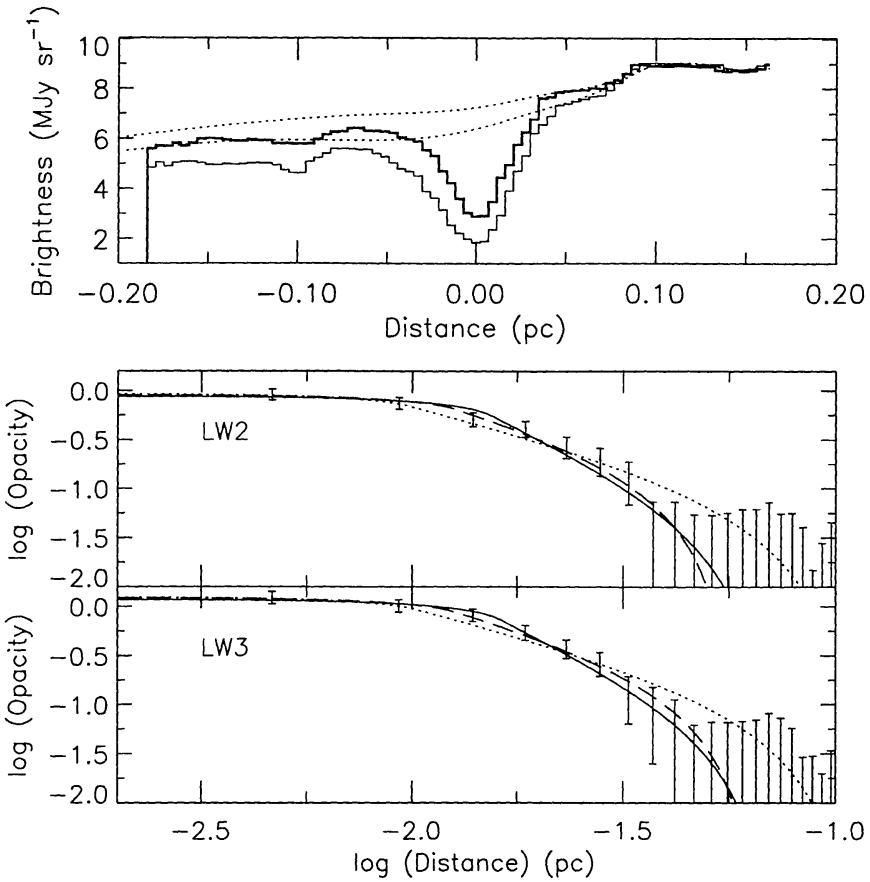

Figure 4. Upper panel: East-west profiles across Oph D at 6.75 μm (thick line) and 15 μm (thin line), after removing the zodiacal emission. A baseline (dotted line) is subtracted before computing the opacity profiles (see the text). Lower panels: Western edges of the opacity profiles for the LW2 and LW3 filters. The dotted and solid lines show the result of our modeling with β= 2 and 3 respectively and an external density n_{out} fixed to 10^4 H cm^{-3}. The dashed line is for β= 2 and n_{out} adjusted. The parameter values are given on table 1.

H cm^{-3}) and a radius r_0 around 10^{-2} pc. Therefore we confirm the systematic central flatenning of starless cores revealed by submillimeter and millimeter observations (Ward-Thompson et al, 1994, André et al, 1996).
In the external parts (typically at r >0.03 pc), the agreement of the fits with the data depends on the external density n_{out}. If n_{out} is fixed to 10^4 cm^{-3}, β= 3 gives a better agreement than β= 2 for the two filters. However, if n_{out} is adjusted together with the other parameters, a comparable agreement is obtained (even better for the LW2 filter, see the χ^2 value in table 1) but n_{out} is found in the range 3-5 10^4 H cm^{-3} for β= 2, while it is still around 10^4 H cm^{-3} for β= 3. This is due to the fact that, for β= 2 and n_{out}= 3-5 10^4 H cm^{-3}, the value of the core radius r_{core} is identical to the value obtained with β= 3 and n_{out}= 10^4 H cm^{-3}. The solid and dashed lines of figure 3, which correspond to the two cases, show similar profiles which both fit with the data.

© Astronomical Society of the Pacific • Provided by the NASA Astrophysics Data System

1998ASPC..132..220A

Table 1. Parameters of the computed profiles of Fig. 3

	n_{out} (H cm^{-3})	r_0 (pc)	n_0 (H cm^{-3})	N_H (H cm^{-2})	χ^2
LW2, β= 2	1 10^4 (1)	0.010	1.2 10^6	1.3 10^{23}	9.6 10^{-3}
LW2, β= 3	1 10^4 (1)	0.015	8.8 10^5	1.2 10^{23}	6.6 10^{-3}
LW2, β= 2	5.1 10^4	0.012	1.0 10^6	1.4 10^{23}	3.3 10^{-3}
LW3, β= 2	1 10^4 (1)	0.010	1.1 10^6	1.3 10^{23}	1.5 10^{-2}
LW3, β= 3	1 10^4 (1)	0.016	8.4 10^5	1.2 10^{23}	3.9 10^{-3}
LW3, β= 2	3.7 10^4	0.012	9.9 10^5	1.4 10^{23}	3.5 10^{-3}

(1) Fixed parameter

7. Conclusion

To derive quantitative parameters from the observation of the extinction across Oph D by ISOCAM in the two filters LW2 and LW3, we first have estimated the foreground emission. This emission is obviously lower than the minimal emission measured in the core, but also higher than the zodiacal emission estimated using the model of Reach et al. 1995 calibrated with DIRBE measurements. Using these constraints, opacity maps have been derived which reveal the complex geometry of the core with a resolution of 6 arcsec. We have used the values of the cross section of dust particles of Draine and Lee (1984) which are consistent with the wavelength dependence of the extinction deduced from our observations. Our estimates of the total mass of the core (M_{TOT}= 7.3-13.9 and 8.4-10.8 $M_\odot$ for the LW2 and LW3 filters respectively) are in agreement with measurements deduced from DCO^+ observations (Butner et al. 1995).
The density structure of the core edge which has the steepest IR brightness gradient clearly departs from a singular r^{-2} law due to a central flatenning of the internal regions. The description of Oph D as a core embedded in an external cloud of density fixed to 10^4 H cm^{-3} (value consistent with the ^{13}CO J=1-0 observations of Loren 1989) leads to the conclusion that the external parts of the western side of the density profiles are steeper than a r^{-2} law. On the other hand, r^{-2} profiles are compatible if the external density is assumed in the range 3-5 10^4 H cm^{-3}. The constraints on the density deduced from the ^{13}CO observations are not very strong. The tri-dimensional geometry of the core is not known, especially at the interface between the core and the external cloud. Therefore it is not possible to definitively rule out r^{-2} profiles to explain the external parts of the extinction profiles across Oph D revealed by ISOCAM data.

References

Abergel A., et al., 1996, A&A 315, L329
André P., Ward-Thompson D., Motte F., 1996, A&A 314, 625
Bacmann et al. 1997, this conference

© Astronomical Society of the Pacific • Provided by the NASA Astrophysics Data System

1998ASPC..132..220A

Benson P.J., Myers P.C. 1989, ApJS 71, 89
Bertiau F.C., 1958, ApJ 128, 533
Butner H.M., Lada E.A., Loren B.R. 1995, ApJ 448, 207
Cesarsky., C.J. et al., 1996, A&A 315, L32
de Geus E.J., Zeeuw P.T., Lub J., 1989, A&A 216, 44
Draine B.T., Lee H.M., 1984, ApJ 285, 89
Falgarone E., Puget J.L., 1985, A&A 142, 157
Greene T.P., Young E.T., 1992, ApJ 395, 516
Henning T. Michel B., Stognienko R., 1995, Planet. Space Sci. 43, 1333
Loren R.B., 1989, ApJ 338, 902
Loren R.B., Wootten A., 1986, ApJ 306, 142
Loren R.B., Wootten A., Wilking B.A., 1990, ApJ 365, 269
Lutz D., et al., 1996, A&A 315, L269
Motte F., André P., Neri R. 1997, submitted to A&A
Myers P.C., Benson P.J. 1983, ApJ 266, 309
Reach W.T et al. 1995. In Dwek E. (ed.) Unveiling the cosmic infrared background. AIP press, New York, p. 37
Reach W.T et al. 1996, A&A 315, L381
Shu F. 1977, ApJ 214, 488
Ward-Thompson D., Scott P.F., Hills R.E., André P. 1994, MNRAS 268, 276
Wilking B.A., Lada C.J., Young E.T. 1989, ApJ 340, 823

© Astronomical Society of the Pacific • Provided by the NASA Astrophysics Data System

1998ASPC..132..220A

Part 6

Jets and Outflows

© Astronomical Society of the Pacific • Provided by the NASA Astrophysics Data System